Frontiers in Bioscience Scholar

Front. Biosci. (Schol Ed) **2022**; 14(4): 30
https://doi.org/10.31083/j.fbs1404030

Original Research

Measurement of the Elastic Modulus of Cornea, Sclera and Limbus: The Importance of the Corneal-Limbus-Scleral Biomechanical Unit

Frederick H. Silver[1,2,*], Tanmay Deshmukh[2], Dominick Benedetto[3], Michael Gonzalez-Mercedes[2], Arielle Mesica[2]

[1]Department of Pathology and Laboratory Medicine, Robert Wood Johnson Medical School, Rutgers, The State University of New Jersey, Piscataway, NJ 08854, USA
[2]OptoVibronex, LLC., Ben Franklin Tech Partners, Bethlehem, PA 18015, USA
[3]Center for Advanced Eye Care, Vero Beach, FL 32960, USA
*Correspondence: silverfr@rutgers.edu (Frederick H. Silver)
Academic Editor: Thomas Heinbockel
Submitted: 12 August 2022 Revised: 22 September 2022 Accepted: 29 September 2022 Published: 3 November 2022

Abstract

Background: Energy storage, transmission and dissipation are important considerations of normal mechanical homeostasis. In this paper we present a new technique termed vibrational optical coherence tomography (VOCT) to study the anterior anatomic structures of the pig eye to better understand how energy applied to the cornea is dissipated without delamination occurring. **Methods**: VOCT uses infrared light and an applied sinusoidal audible sound wave to image and measure the resonant frequency and modulus of individual macromolecular components of tissue non-invasively. We have measured the resonant frequencies and calculated the moduli of tissues in the anterior portion of the pig eye using VOCT. **Results**: While both pig and human eyes have similar resonant frequencies, they do differ in the peak amplitudes near the frequencies of 80, 120, 150 and 250 Hz. It is known that the stroma of pig cornea is much thicker than that of human corneas and these differences may explain the normalized peak height differences. The similarity of the resonant frequency peaks near 80, 120, 150 and 250 Hz of cornea, sclera and limbus suggest that the anatomically described layers in these tissues are connected into a single biomechanical unit that can store external mechanical energy and then transmit it for dissipation. Since the energy stored and dissipated is proportional to the modulus and the ability of the tissue to deform under stress, energy storage in these tissues is related to the stiffness. **Conclusions**: It is concluded that stored energy is transmitted to the posterior segment of the eye for dissipation through the attachment with the sclera. This mechanism of energy dissipation may protect the cornea from changes in shape, curvature, and refractive power. However, ultimately, energy dissipation through thinning of the sclera may cause globe elongation observed in subjects with myopia and glaucoma.

Keywords: cornea; sclera; limbus; collagen fibrils; biomechanics; energy storage; energy dissipation; corneal-limbus-scleral biomechanical unit

1. Introduction

Energy storage, transmission and dissipation are important functions of mammalian tissues that are involved in locomotion, pulmonary function and blood flow, tissue mechanical stability, and normal vision. On earth, all tissues experience an external pressure of 1 atmosphere which is equivalent to approximately 760 mm of Hg. This pressure must be offset by internal forces within the tissue or else tissues like skin would rapidly sag and the cornea would flatten. The loss of gravity has been shown to cause the globes of astronauts to flatten, the optic nerve length to change, and result in modification of the location of the optic nerve head [1,2]. The purpose of this paper is to attempt to understand how internal and external mechanical forces affect energy storage and dissipation in the cornea and anterior segment of the eye. This information is needed to understand the changes that occur with aging and disease.

The relationship between energy storage, transmission and dissipation has been studied in several tissues including in muscle and tendon. The muscle-tendon unit is an important example of how energy is generated by muscle, stored in the elastic tendons, transmitted to the joint to promote movement, and then transmitted back through tendon to muscle where it is dissipated [3]. Elastic recoil, primarily by tendons, converts most of the stored energy back to kinetic energy. A study in horses suggests that the muscle–tendon unit not only stores energy during extension, but it also dissipates the energy after extension is complete [4].

In skin, internal tension is supplied by the collagen fibers directed along Langer's lines and by the cells attached to the collagen fibers [5]. This tension prevents tearing of the skin within its plane as well as providing a means of up-regulating cellular mechanotransduction when an external load is applied [6]. In many ways the skin acts as a trampoline by distributing the stress applied to it by external forces.

In articular cartilage, the top layer is stretched in tension over the underlying subchondral bone and acts like a drumhead to redistribute compressive loads across the sur-

face of the joint [7]. The applied energy is partially dissipated through viscous movement of fluid in and out of the cartilage as well as by viscous sliding of collagen fibers by each other during cartilage deformation [7]. Cartilage recovery after unloading occurs due to osmotic forces that lead to rehydration of the collagen-proteoglycan matrix.

While energy storage, transmission and dissipation have been addressed in these tissues very little attention has been paid to how energy is stored, transmitted, and dissipated in the eye. While the cornea is the major tissue that protects the visual components in the anterior and posterior segments of the eye from mechanical damage, it is in series mechanically with the sclera and limbus. In addition, other forces acting on the cornea include atmospheric pressure, gravity, lid pressure, intraocular pressure, muscular forces, and surface tension from the tear film. Therefore, it is important to understand how forces applied to the cornea and corneal stiffness impact energy storage and dissipation in the eye. Even though the cornea is a multilayered structure, it does not delaminate when it is overstressed *in vivo*.

The purpose of this paper is to present the results of a pilot study using vibrational optical coherence tomography (VOCT) to determine the elastic moduli of different components of the anterior chamber of the eye in both excised globes and in selective isolated eye tissues. The elastic modulus is related to the energy stored in a material [6,7]. These results are needed to be able to speculate on how these structures store, transmit and dissipate energy applied to the cornea. Of primary concern is how the cornea, a multilayered structure, stores, transmits and dissipates energy without delaminating or tearing.

2. Materials and Methods

2.1 Measurement of Ocular Component Stiffness

Optical coherence tomography is a technique that uses infrared light that is reflected to a detector from different depths in a tissue to create an image. By applying an acoustic force and measuring the change in displacement of the tissue, it is possible to measure the tissue stiffness [8,9]. The weighted displacement of a tissue is obtained after correction for the displacement of the speaker and out of phase vibrations (viscoelasticity) as a function of frequency. The human mechanovibrational spectra of corneas from 20 normal control subjects were previously reported [10]. They were used in this study for comparison with the measurements made on fresh whole pig eyes. The pig eyes were studied intact as well as after the cornea, lens and iris were dissected away from the remaining components of the eyes. 15 fresh pig eyes were obtained from Spear products (Coopersburg, PA, USA) and kept on ice during transport for testing. The pigs weighed 220 to 280 lbs and were 6 to 12 months old. Pig eyes were studied using vibrational optical coherence tomography (VOCT) within 4 hours of harvesting at Ben Franklin Tech Ventures (Bethlehem, PA, USA). It was noted the cornea thickness increased within several hours of harvesting the eyes even when the eyes were kept on ice.

2.2 OCT Images

OCT image collection was accomplished using a Lumedica Spectral Domain OQ 2.0 Labscope (Lumedica Inc., Durham, NC, USA) operating in the scanning mode at a wavelength of 840 nm. The device generates a 512 $\times$ 512 pixel image with a transverse resolution of 15 micrometers and an A-scan rate of 13,000/sec. All gray scale OCT images were color coded to enhance the image details. The images were used to locate exactly where the VOCT measurements were made.

2.3 Measurement of Resonant Frequency and the Elastic Modulus

The OQ Labscope was modified by adding a speaker 2 inches in diameter (A106 Pro, JYM Electronics Co., Ltd, Shajing Town, China) to vibrate the tissue at 55 dB sound pressure density in the VOCT studies [9–12]. The Labscope was also modified to collect and store single unprocessed raw OCT image data that was used to calculate sample displacements (amplitude information) from amplitude line data. The data was processed using MATLAB software R2020a version 9.8 (Mathworks, Natick, MA, USA) as discussed previously [12,13]. The displacement of the tissue is detected by measuring the frequency dependence of the deformation based on the reflected infrared light and filtered to collect only vibrations that were in phase (elastic component) with the sound input. The vibrations for each frequency were collected and stored on the cloud for further analysis as a mechanovibrational spectrum. The mechanovibrational spectral peaks were normalized by dividing by the largest peak in each spectrum to correct for speaker orientation and varying sound levels that occur during data collection on different samples.

The resonant frequency of a tissue component is defined as the frequency at which the maximum in-phase displacement is observed in the amplitude data. The measured resonant frequencies are converted into elastic modulus values using a calibration equation (Eqn. 1) developed based on *in vitro* uniaxial mechanical tensile testing and VOCT measurements made on the same tissue at the same time as reported previously [8–13]. The resonant frequency of each sample is determined by measuring the displacement of the tissue resulting from transversely applied sinusoidal audible sound driving frequencies ranging from 30 Hz to 300 Hz, in steps of 10 Hz. Since the measurements were made at 10 Hz steps the resonant frequencies were observed to occur at intervals of +/- 10 Hz. For this reason, the location of the peaks on some of the samples differ by as much as 20 Hz. The peak frequency (the resonant frequency), f_n, is defined as the frequency at which the displacement is maximized after the vibrations due to the speaker are removed.

$$E \times d = 0.0651 \times \left(fn^2\right) + 233.16 \qquad (1)$$

Since soft tissues have a density very close to 1.0, Eqn. 1 is valid for most tissues found in the body; where the thickness d is in m and is determined from OCT images, fn^2 is the square of the resonant frequency, and E is the tensile elastic modulus in MPa as discussed previously [8–13]. Eqn. 1 was used to calculate the modulus values and is an empirical equation based on calibration studies using decellularized human skin (dermal collagen) tested in uniaxial tension and simultaneously by VOCT [8–13]. The elastic modulus measured using VOCT is a materials property at low strains since the viscous component of the behavior is only 2% to 3% of the total modulus at the resonant frequency [14] and the modulus is unchanged at strains less than about 7% for collagenous materials [14].

Pig eye studies were conducted *in vitro* using a microscope stand on which the tissue to be examined was placed [12,13]. Whole pig eyes were examined after the fat, orbital muscles and conjunctiva were removed by dissection. The cornea, sclera, limbus, and lens were studied in the intact eye; the eye was then dissected, and the cornea, lens, and iris were excised for VOCT measurements.

All resonant frequencies and moduli were compared using a paired two tailed Student's *t*-test. All differences were considered statistically significant if the *p* value was at a 0.05 level or less.

3. Results

VOCT data was collected on whole pig eyes after which the cornea, lens, and iris were dissected from the eyes. Fig. 1 (Ref. [10]) shows a normalized plot of weighted displacement versus frequency for a typical human normal control cornea collected *in vivo* and reported previously [10]. The data was normalized by dividing the weighted displacements by the largest weighted peak in the mechanovibrational spectrum. Note major resonant frequency peaks exist at 70, 120, 150, and 250 Hz.

When whole pig eyes were studied *in vitro* after dissection of the surrounding fat, extraocular muscles and conjunctiva, peaks were observed in the mechanovibrational spectrum that occurred at similar frequencies to those observed in human eyes *in vivo*. Fig. 2 shows a plot of normalized weighted displacement versus frequency for a typical pig globe measured *in vitro*. Note the major resonant frequency peaks at 80, 110, 150 and 250 Hz. These peaks are like those reported for human eye [10] and suggest that although pig corneas are thicker than human corneas, they have similar component resonant frequencies.

Pig corneas isolated by dissection show similar peaks to those seen in intact pig globes. Fig. 3 shows a typical plot of normalized weighted displacement versus frequency for an excised pig cornea measured *in vitro* with the anterior

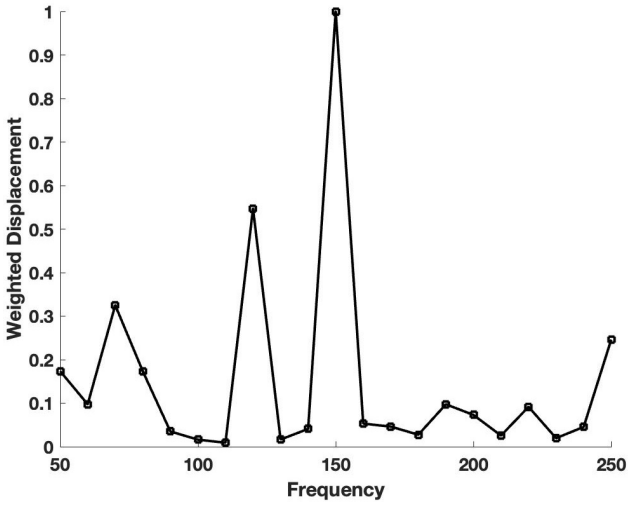

Fig. 1. Plot of weighted displacement versus frequency for human corneas. A normalized plot of weighted displacement versus frequency for a typical human normal control cornea collected *in vivo* is shown. The data was normalized by dividing the weighted displacements by the largest weighted displacement peak in the mechanovibrational spectrum. The raw data were previously reported [10] and recalculated in this study. Note the major resonant frequency peaks at 70, 120, 150, and 250 Hz.

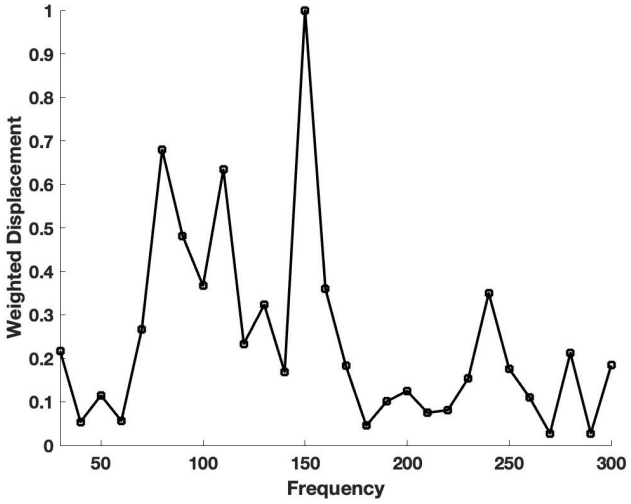

Fig. 2. Plot of weighted displacement versus frequency for pig globes. A plot is shown of normalized weighted displacement versus frequency for a typical pig globe measured *in vitro* after extraneous tissue and the conjunctiva were removed. Note the major resonant frequency peaks at 80, 110, 150 and 250 Hz similar to human cornea shown in Fig. 1.

side up to the light beam (A), the posterior side up (B) and part of the anterior surface removed (C). Note the presence of resonant frequency peaks at 85–90, 110, 150 and 240–250 Hz suggesting that there are several different structures that resonate in different layers of the cornea. Removing part of the anterior segment of the cornea does not com-

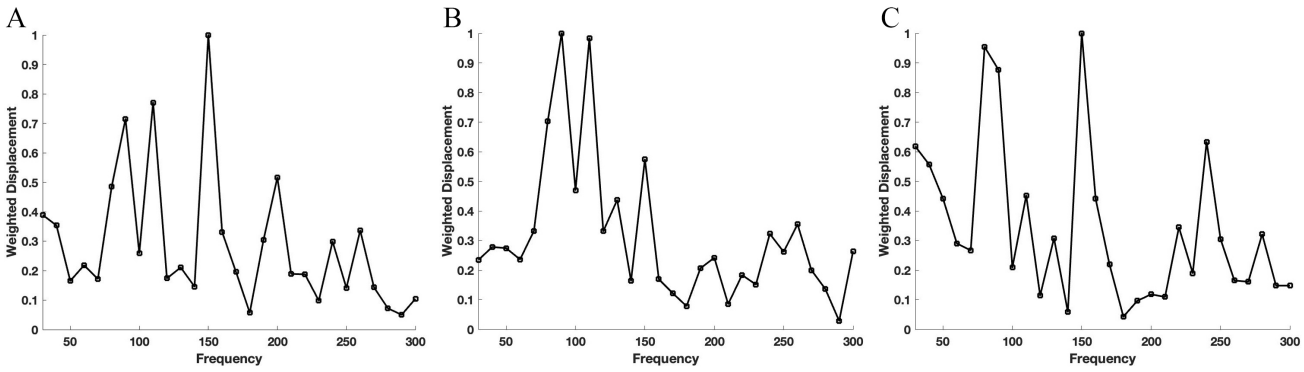

Fig. 3. Weighted displacement versus frequency for pig cornea. Typical plots of normalized weighted displacement versus frequency for an excised pig cornea measured *in vitro* with the anterior side facing up to the light beam (A), the posterior side facing up (B) and after removing part of the anterior side by dissection (C). There are several different structures that resonate in the cornea at frequencies between 85–90, 110–120, 150 and 240–250 Hz that are found in different layers of the cornea.

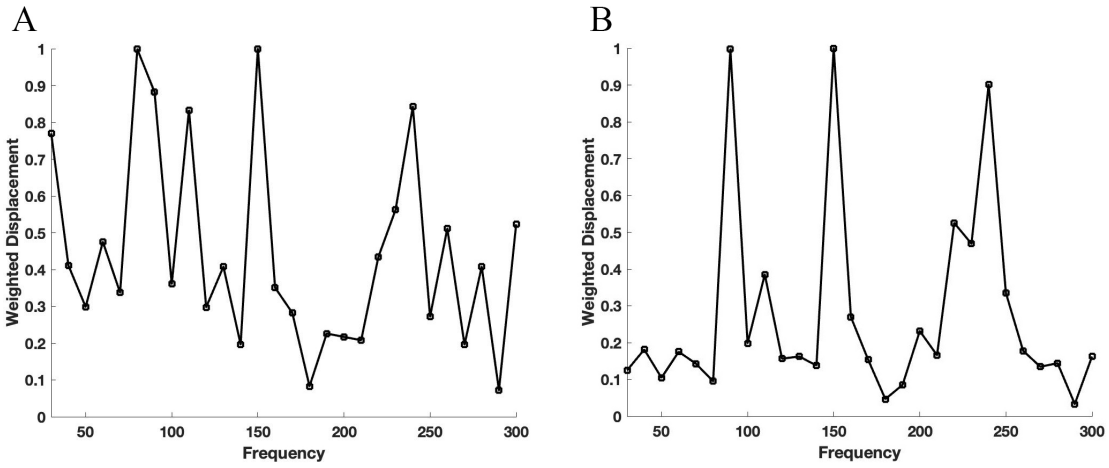

Fig. 4. Weighted displacement versus frequency for pig sclera. A typical plot of normalized weighted displacement versus frequency for a pig sclera measured *in vitro* in in the anterior (A) and posterior (B) segments of the eye is shown. Note the peaks shown at about 80 Hz (80–90 Hz), 110, 150 and 240 Hz (240–250 Hz).

pletely remove any of the peaks (Fig. 3C). The peak heights are compared in Fig. 4. Note the changes in the peak heights after the different corneal treatments. The peak height at 85–90 Hz for human cornea is statistically different at a 0.95 confidence level using a paired two tailed Student's t test to the resonant frequency peak heights for pig corneas and limbus while the peak at 240–250 Hz is statistically different at a 0.95 confidence level for pig limbus compared to all the other specimen tested. The major difference between pig cornea and limbus is that the limbus has a higher ratio of the stiffer 240–250 Hz peak.

Pig sclera has similar peaks compared to pig cornea. Fig. 4 shows a typical plot of normalized weighted displacement versus frequency for a pig sclera measured on a whole eye *in vitro* in the anterior (A) and posterior areas of the eye (B). Note the peaks at 80–90, 110–120, 150 and 240–250 Hz are like the peaks seen in pig cornea, sclera, and limbus.

Fig. 5A shows a bar graph comparing the elastic modulus values for human and pig corneas and pig limbus. Note the human tissues are stiffer than pig tissues at a 95% confidence level and may reflect the differences in corneal thicknesses, which are about 0.55 mm on average in humans [14], versus about 1.13 mm thick on average in pigs [15]. Fig. 5B illustrates that pig anterior and posterior sclera elastic moduli are the same and are not statistically different.

Typical plots of elastic moduli for pig cornea, sclera, iris, limbus and lens are shown in Fig. 6. Note iris and lens are stiffer at all frequencies compared to cornea, sclera and limbus at a 0.95 confidence level based on a paired two tailed paired Student's *t* test. The statistical data comparisons for resonant frequencies and moduli are shown in Tables 1,2,3 and 4.

4. Discussion

Collagenous tissues in the eye including the cornea, sclera and limbus are viscoelastic materials that have moduli that are strain-rate and strain dependent except at or above the resonant frequency [14]. At or above the resonant

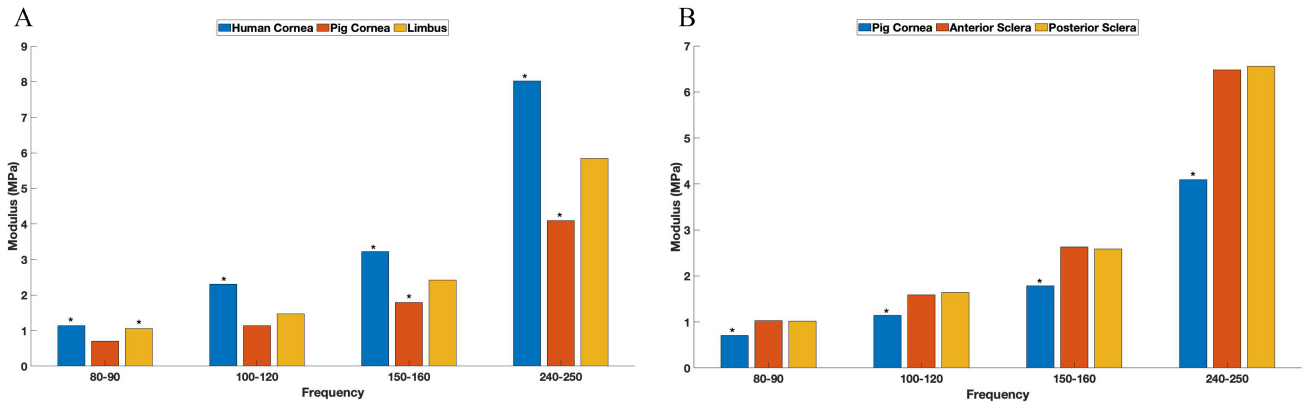

Fig. 5. Modulus values for human and pig corneas. The bar graph shows a comparison between the elastic modulus values for human and pig corneas and pig limbus (A) and cornea and sclera (B). Note the asterisks denote values that are significantly different at the 0.95 confidence level. Note the resonant frequencies depicted at 80 Hz actual represent values determined from 80 to 95 Hz, while the ones depicted at 250 were collected from 240–250 Hz.

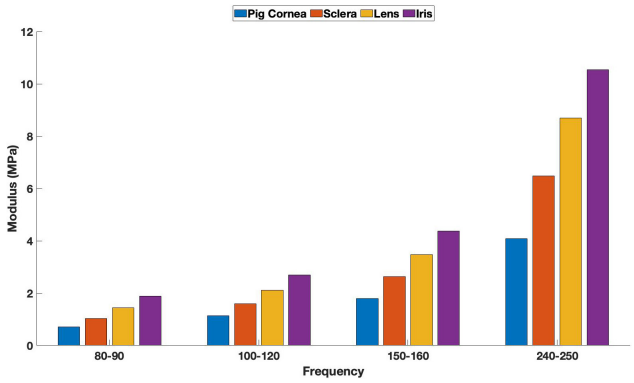

Fig. 6. Elastic moduli for pig cornea, sclera, iris and lens. The elastic moduli of iris and lens at 250 Hz is seen to be significantly higher than the modulus of cornea and sclera at a 0.95 confidence level. Note the resonant frequencies depicted at 80 Hz actual represent values determined from 80 to 95 Hz, while the ones depicted at 250 were collected from 240–250 Hz.

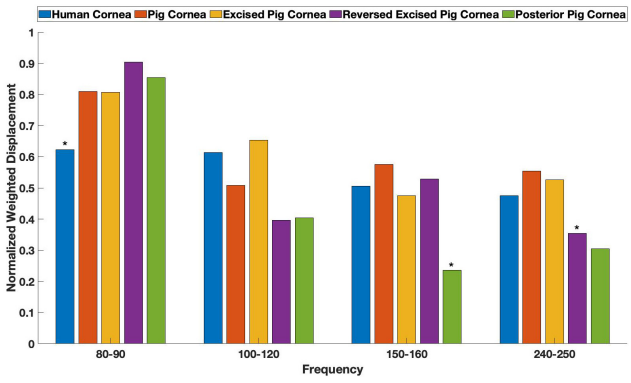

Fig. 7. Bar graph comparing normalized weighted displacement versus frequency for pig cornea. A comparison of pig cornea (excised cornea), reversed excised pig cornea (posterior side up) and excised posterior cornea (posterior cornea only) is shown. Note the changes in peak heights after the different corneal treatments. The resonant frequencies depicted at 80 Hz actual represent values determined from 80 to 95 Hz, while the ones depicted at 250 were collected from 240–250 Hz.

frequency collagenous materials are almost purely elastic and the modulus measured is a materials constant at low strains [14]. Therefore, measurements of the modulus using VOCT reflect the elastic behavior of the tissue and the energy storage capabilities of the tissue.

The components of the anterior compartment of the eye include the cornea, sclera, lens, and iris. Each of these tissues are multi-layered; each layer contributes to the resonant frequencies measured using VOCT. In this study we measured the resonant frequencies seen in pig whole eyes as well as the resonant frequencies of components of the anterior segment that could be isolated by dissection. Each of these tissues exhibit resonant frequencies in the ranges of 80–95, 110–120, 150 and 240–250 Hz. Previously, it has been reported that the 80 Hz peak is associated with the cellular components, the 120 and 150 Hz peaks probably represent the collagen in the posterior and anterior stroma lamellae, and the 250 Hz peak probably represents fibrous tissue [10,12,13]. Therefore, it is important to understand the composition and mechanical behavior of each of the tissues in the anterior compartment. The peak heights measured in human eyes were higher than those observed in the pig eyes, possibly due to differences in corneal thickness. The average pig central cornea thickness is about 2.06 times the thickness of the human central cornea.

4.1 VOCT Results for Cornea

Our previous published results [10] suggest that the mechanovibrational spectrum of human cornea *in vivo* has peaks at 80, 120, 150 and 250 Hz (Figs. 1,7) which is similar to those found in the central cornea of pig eyes *in vitro* (Fig. 2). The cornea is made up of cellular and acellular

Table 1. Statistical significance of the VOCT peak heights for pig cornea (whole eye), excised pig cornea, reversed excised pig cornea, and posterior side of pig cornea.

80–90 Hz				
	Pig Cornea	Excised Pig Cornea	Reversed Excised Pig Cornea	Posterior Pig Cornea
Human Cornea	0.02	0.03	0.019	0.02
Pig Cornea	NA	0.49	0.23	0.35
Excised Pig Cornea		NA	0.22	0.34
Reversed Excised Pig Cornea			NA	0.35
Posterior Pig Cornea				NA
100–120 Hz				
	Pig Cornea	Excised Pig Cornea	Reversed Excised Pig Cornea	Posterior Pig Cornea
Human Cornea	0.07	0.34	0.12	0.14
Pig Cornea	NA	0.08	0.26	0.29
Excised Pig Cornea		NA	0.09	0.11
Reversed Excised Pig Cornea			NA	0.48
Posterior Pig Cornea				NA
150–160 Hz				
	Pig Cornea	Excised Pig Cornea	Reversed Excised Pig Cornea	Posterior Pig Cornea
Human Cornea	0.26	0.38	0.43	0.03
Pig Cornea	NA	0.23	0.39	0.02
Excised Pig Cornea		NA	0.37	0.06
Reversed Excised Pig Cornea			NA	0.06
Posterior Pig Cornea				NA
240–250 Hz				
	Pig Cornea	Excised Pig Cornea	Reversed Excised Pig Cornea	Posterior Pig Cornea
Human Cornea	0.19	0.30	0.03	0.20
Pig Cornea	NA	0.40	0.01	0.12
Excised Pig Cornea		NA	0.04	0.15
Reversed Excised Pig Cornea			NA	0.39
Posterior Pig Cornea				NA

The data was analyzed using a paired two tailed Student's *t*-test. All data with a *p* value of less than 0.05 is significantly different and is shown in bold numbers.

components. The cellular components include the epithelial cells, keratocytes, and endothelial cells [15] and appear to contribute to the 80 Hz peak. The acellular components of the cornea include collagen and glycosaminoglycans that make up the stroma and tangentially oriented collagen fibrils at the corneal-limbus interface of the human eye [16,17]. There are 200 to 250 distinct lamellae in the stroma; each layer is arranged at right angles relative to fibers in adjacent lamellae. Anterior corneal stromal rigidity appears to be particularly important in maintaining the corneal curvature [18]. However, these lamellae must be connected or else they could easily be peeled away from each other under mechanical loading. Based on our VOCT results it is hypothesized that the 150 Hz peak may represent the anterior cornea collagen fibrils since it has been reported that the anterior layers have a lamellar density some 50% greater than those in the deep layers [19]. These layers may contribute to the diamond shaped pattern of the interface between the collagen fibrils of the limbus and stroma proposed [18–20]. It is postulated that the 120 Hz peak represents the collagen fibrils of the posterior lamellae; these must be connected to the fibrils in the anterior lamellae to form a continuous mechanical network or separation of the layers would occur under mechanical loading. The 250 Hz peak may represent vibrations from the corneal-scleral junction (limbus) where the collagen fibrils from the limbus are believed to fuse with the corneal lamellae (see Fig. 8 for a model). Since the sclera and cornea fuse at the limbus, the stiffness of these components must be similar to prevent modulus mismatches that could lead to mechanical failure at the interfaces between the cornea and limbus and the limbus and sclera.

The limbus is thought to stabilize the cornea with a diamond shaped pattern of collagen fibrils that run in a circumferential direction [17–19]. In the model presented in this figure it is proposed that covalent connections exist between collagen fibrils in the cornea, and collagen fibrils and fibers in the limbus. This linkage is required to prevent de-

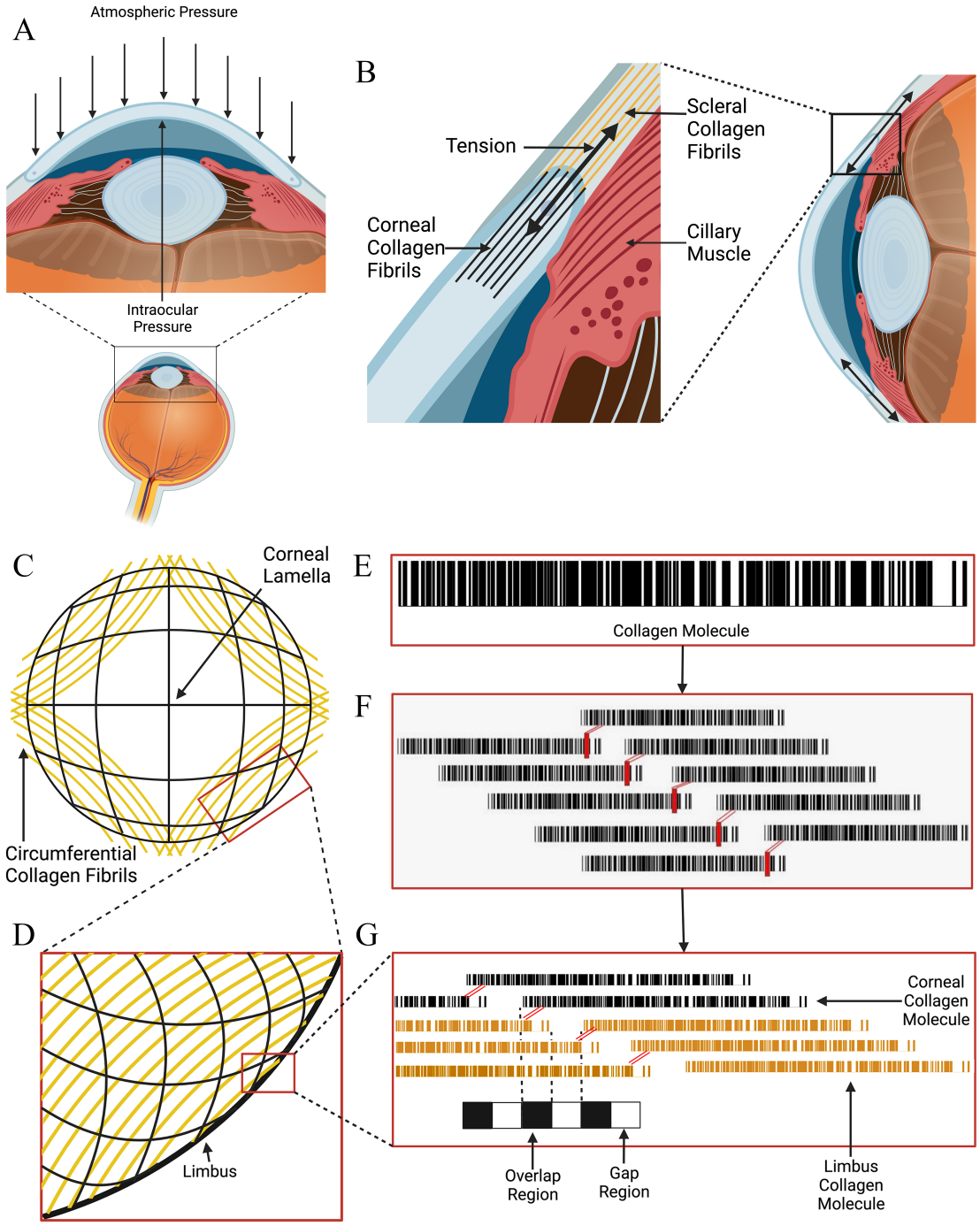

Fig. 8. Diagrammatic representation of the forces acting on the eye. This diagram illustrates the connections between collagen fibrils in the cornea and limbus that stabilize the corneal-limbus-scleral junction. The forces acting on the eye include the force of gravity, atmospheric pressure (A), tension in the sclera (B), lid pressure (not shown), the forces due to the orbital muscles (not shown), ciliary muscle (in the non-accommodation mode not shown), atmospheric pressure, and intraocular pressure. Hypothetical model of arrangement of collagen fibrils in the cornea (C), and limbus (D). The collagen molecule with its rigid and flexible regions is shown in E, the microfibril in (F) and crosslink connections between collagen fibrils of the limbus and cornea (G) that are part of the cornea-limbus-sclera mechanical unit that stabilizes the cornea from changes in size and shape during aging and mechanical loading. The collagen molecule in E is depicted as a series of light and dark bands that represent the flexible (light) and rigid (black) amino acid sequences in type I collagen that line up in register to form quarter-staggered microfibrils shown in F containing 5 molecules in cross-section and a longitudinal hole region. G shows an enlarged model showing that the connections between collagen fibrils in the limbus and cornea are stabilized by end-overlap crosslinks that form a continuous mechanical network.

Table 2. Statistical significance of the VOCT peak heights for human cornea, excised pig cornea and limbus.

80–90 Hz Moduli		
	Pig Cornea	Pig Limbus
Human Cornea	0.000003	0.26
Pig Cornea	NA	0.01
Pig Limbus		NA
100–120 Hz Moduli		
	Pig Cornea	Pig Limbus
Human Cornea	0.0001	0.0009
Pig Cornea	NA	0.056
Pig Limbus		NA
150–160 Hz Moduli		
	Pig Cornea	Pig Limbus
Human Cornea	0.0001	0.001
Pig Cornea	NA	0.01
Pig Limbus		NA
240–250 Hz Moduli		
	Pig Cornea	Pig Limbus
Human Cornea	0.0000002	0.01
Pig Cornea	NA	0.02
Pig Limbus		NA

The data was analyzed using a paired two tailed Student's *t*-test. All data with a *p* value of less than 0.05 is significantly different.

Table 3. Statistical significance of the VOCT peak heights for pig cornea (whole eye), anterior sclera, and posterior sclera.

80–90 Hz Moduli		
	Anterior Sclera	Posterior Sclera
Pig Cornea	0.0005	0.001
Anterior Sclera	NA	0.46
Posterior Sclera		NA
100–120 Hz Moduli		
	Anterior Sclera	Posterior Sclera
Pig Cornea	0.009	0.02
Anterior Sclera	NA	0.40
Posterior Sclera		NA
150–160 Hz Moduli		
	Anterior Sclera	Posterior Sclera
Pig Cornea	0.002	0.003
Anterior Sclera	NA	0.40
Posterior Sclera		NA
240–250 Hz Moduli		
	Anterior Sclera	Posterior Sclera
Pig Cornea	0.0001	0.01
Anterior Sclera	NA	0.44
Posterior Sclera		NA

The data was analyzed using a two tailed Student's *t*-test. All data with a *p* value of less than 0.05 is significantly different.

lamination of these structures during mechanical loading. The model is an extension of the models described by Silver *et al*. [30] and was created using Biorender.com.

4.2 Sclera

The sclera protects the intraocular structures from mechanical damage as well as prevents light scattering in the eye due its opacity from distorting the retinal image [21]. It is composed of several layers including tenon's capsule, episcleral, stroma and a perilimbal layer where it interfaces with the limbus [17]. At its anterior boundary the sclera merges with the corneal perimeter at the limbus and extends backward to approximately form a sphere. At the back of the eye, the scleral connective tissue fuses with the dural sheath of the optic nerve [17].

Episclera is a dense layer of collagen found in bundles that run circumferentially around the eye and merge with the underlying stroma [17]. They prevent radial enlargement of the sclera due to increases in internal pressure in the eye by limiting "hoop strain" preventing "blow out" failure of the globe [21–23]. It merges with the superficial layer of the limbus and therefore should have a similar modulus to that layer. The episcleral and stroma merge together to form a continuous interface.

Stroma contains bundles of parallel-aligned individual collagen fibrils with diameters 25–230 nm, interspersed in places with elastic microfibrils and fibers. They form lamellae 0.5–6 μm thick that lie roughly in the plane of the eyeball surface [17]. Scleral lamellae overall demonstrate far more branching and interweaving than those of the corneal stroma, and the extent of this varies with both tissue depth and anatomical location [24]. Superficially, the scleral collagen fibril bundles merge with tenon fibers at the extraocular muscle insertion sites, while in the deepest stromal layers adjacent to the uvea they taper and branch to intermingle with the underlying choroid [17]. Since the stroma of the sclera intersects the limbus, this may explain the peaks at 120 and 150 Hz seen in both tissues.

While the organization of sclera is clearly different from that of the cornea, it exhibits similar resonant frequencies due to cells (80 Hz) and collagen fibrils that merge with the limbus and tenon fibers (120 and 150 Hz). The 150 Hz peak may represent the superficial collagen fibers that merge with the extraocular muscle tendon fibers while the 120 Hz peak may represent the behavior of the deeper collagen lamellae. The 250 Hz peak may also represent the interface with the limbus which is characterized by a similar large peak at that frequency. The increased stiffness of the limbus stabilizes the scleral-limbus-corneal junction and limits changes in shape, curvature and refractive power of the cornea during aging, space flight and accommodation.

Table 4. Statistical significance of the VOCT peak heights for pig cornea (whole eye), pig sclera, pig iris and pig lens.

80–90 Hz Moduli				
	Cornea	Sclera	Lens	Iris
Cornea	NA	0.00005	0.0000001	0.001
Sclera		NA	0.00004	0.005
Lens			NA	0.04
100–120 Hz Moduli				
	Cornea	Sclera	Lens	Iris
Cornea	NA	0.009	0.0001	0.001
Sclera		NA	0.0004	0.007
Lens			NA	0.004
150–160 Hz Moduli				
	Cornea	Sclera	Lens	Iris
Cornea	NA	0.002	0.00004	0.002
Sclera		NA	0.0000007	0.01
Lens			NA	0.007
240–250 Hz Moduli				
	Cornea	Sclera	Lens	Iris
Cornea	NA	0.0001	0.0000002	0.001
Sclera		NA	0.0003	0.008
Lens			NA	0.004

The data was analyzed using a paired two tailed Student's *t*-test. All data with a p value of less than 0.05 is significantly different.

4.3 Limbus

The limbus forms the border separating the cornea, conjunctiva, sclera, and uvea [24]. It contains the pathways for aqueous humor outflow and supports epithelial progenitor movement to maintain corneal epithelial integrity [24–26]. Central to the anterior limbal cribriform layer, radial strands of collagen are found to connect the peripheral cornea to the limbus. These presumed anchoring fibers have both collagen and elastin and are found more extensively in the superficial layers than deep layers [24–27]. The excess of circumferential fibrils in the limbus, based on the change in curvature in the surface of the eye at the limbus, appear to take the form of a well-defined annulus [20]. The 250 Hz peak for pig limbus is significantly higher compared to cornea and sclera suggesting that this peak represents the annulus shaped ring of stiff collagen fibers that occurs at the interface between the sclera and cornea. This ring of collagen fibers not only stabilizes the interface between cornea and sclera, but it also limits transfer of stresses and the resulting deformation of the limbus from the forces generated by the extraorbital muscles during eye movement. The presence of cells (80 Hz) and collagen fibrils that connect to the surface of the cornea (150 Hz peak) and deeper layers of cornea (120 Hz) provide for mechanical continuity between the cornea and sclera. The 250 Hz peak probably reflects the fusion of annular collagen fibrils and the collagen lamellae at the limbus as modeled in Fig. 8. Thinning associated with highly myopic eyes occurs in the sclera and not at the limbus or cornea. This suggests that mechanical loading and increases in the axial length of the globe do not lead to mechanical failure at the interface with the limbus but lead to mechanical "creep" of scleral tissue.

4.4 Lens and Iris

The lens and iris are compositionally different than the sclera, cornea, and limbus. The lens is composed of a high concentration of proteins termed crystallines and is surrounded by a collagenous capsule composed of type IV collagen, laminin, and other macromolecules [28]. The iris is composed of the anterior and posterior leafs with the anterior leaf consisting of loose connective tissue, blood vessels, melanocytes and fibroblasts. The posterior leaf contains the dilator and sphincter muscles and posterior epithelium [29].

It is curious that both tissues exhibited resonant frequency peaks at about 80, 120, 150 and 250 Hz similar to the cornea, sclera and limbus suggesting that all the tissues in the anterior part of the eye appear to be mechanically similar. Modulus matching of the layers in the different components of the eye may provide a manner that energy can be stored and transmitted efficiently without stiffness mismatches or excessive dissipation in any one structure. Modulus mismatches in tissues with implants leads to intimal hyperplasia in arteries and hernia implant failures in humans [11]. The stiffness for both iris and lens at 250 Hz were significantly higher at a 0.95 confidence level than in the cornea and sclera and may reflect the stiff crystalline proteins in the lens and the muscular tissue in the iris.

4.5 Energy Storage, Transmission and Dissipation in the Anterior Portion of the Eye

The cornea, sclera and limbus have been considered individual anatomic structures based on histology and microscopic anatomy. The observation that blunt mechanical trauma, globe elongation, scleral thinning in myopia, and corneal ballooning and rupture in keratoconus do not result in delamination of any of these components suggests that the cornea, limbus and sclera are one biomechanical unit. The fact that these structures are composed of layers of tissue that are integrated together suggests that forces applied, and energy stored in any of these anatomic structures is eventually transmitted to the back of the sclera and the posterior chamber. Forces applied to the eye including gravity, eye lid pressure, surface tension, orbital muscle tension, intraocular pressure, and ciliary muscle tension all affect the corneal-limbal-scleral biomechanical unit. The cornea-limbus-sclera biomechanical unit may involve self-assembly and crosslinking of collagen molecules at the limbus into a reinforcing network similar to that seen in tendon [30] as diagrammed in Fig. 8. Each of these tissues has components with resonance frequencies of about 80, 120,

150 and 250 Hz that are involved in cellular events during mechanotransduction (peak at 80 Hz), transmission of mechanical loading information through the collagen network (peaks at 120 and 150 Hz) and prevention of premature mechanical failure (peak at 250 Hz). The importance of the coordination of these structures in maintaining corneal curvature is essential to maintaining normal vision. Any change in corneal shape or curvature induced by mechanical loading would alter the ability to see. Scleral thinning and globe elongation while altering the focal point of light on the retina do not alter the ability to correct for these changes. The ability of the cornea-limbus-scleral mechanical unit to store energy through elastic deformation and transfer it back through the sclera to the posterior chamber provides a means to maintain correction and maintain normal vision. It is only when the energy transmitted back to the posterior chamber through the sclera causes permanent alteration of the tissues in the posterior chamber that normal vision is threatened. It is important in future studies to consider if changes in the corneal-limbal-scleral biomechanical unit may be involved in the development of myopia and glaucoma especially if the sclera thins excessively with age.

4.6 Limitations

The limitations of the study include the inability of being able to separate by dissection the anterior and posterior parts of the sclera. Future measurements on isolated layers of the sclera, limbus and cornea are needed to understand how each of the layers contribute to the mechanical properties of the whole tissues.

5. Conclusions

We have measured the resonant frequency and calculated the modulus of tissues in the anterior portion of the pig eye. While both pig and human eyes have similar resonant frequencies, they do differ in the amplitudes of the peaks near 80, 120, 150 and 250 Hz. It is known that pig corneas are much thicker than human corneas and these differences may explain some of the normalized peak height differences. The similarity of the resonant frequency peaks near 80, 120, 150 and 250 Hz of the different structures in the eye suggest that the anatomical layers in the cornea, limbus and sclera are connected into a single biomechanical unit that can store external mechanical energy and then transmit it for dissipation. It is proposed that the energy applied to the cornea is transmitted to the posterior segment of the sclera through the stiff cornea-limbus-scleral junction. This mechanism of dissipation appears to protect the cornea from changes in shape, curvature, and refractive power required that could not be corrected using either lasers, glasses or contact lenses.

Availability of Data and Materials

Data is available at https://optovibronex.com/.

Author Contributions

Conceptualization—FHS, DB, TD and MGM; methodology—TD, MGM and AM; formal analysis—MGM, DB and FHS; investigation—TD, MGM and AM; data curation—TD, AM, MGM; writing - original draft preparation—FHS and DB; writing - review and editing—DB, MGM, AM and FHS. All authors have read and agreed to the published version of the manuscript.

Ethics Approval and Consent to Participate

All human data was compiled and published previously [10]. That prospective study was complied with the Health Insurance Portability and Accountability Act, adhered to the tenets of the Declaration of Helsinki, and was approved by the Wills Eye Hospital Institutional Review Board (IRB#2021-36). All participants provided informed consent prior to inclusion in the study.

Acknowledgment

The Authors would like to thank Jose Pulido for assistance with collecting parts of the pig eyes.

Funding

This research received no external funding.

Conflict of Interest

FHS is a stockholder of OptoVibronex, LLC. TD, MGM and AM are employees of OptoVibronex, LLC.

References

[1] Huang AS, Stenger MB, Macias BR. Gravitational Influence on Intraocular Pressure. Journal of Glaucoma. 2019; 28: 756–764.

[2] Wåhlin A, Holmlund P, Fellows AM, Malm J, Buckey JC, Eklund A. Optic Nerve Length before and after Spaceflight. Ophthalmology. 2021; 128: 309–316.

[3] Roberts TJ, Marsh RL, Weyand PG, Taylor CR. Muscular Force in Running Turkeys: The Economy of Minimizing Work. Science. 1997; 275: 1113–1115.

[4] Wilson AM, McGuigan MP, Su A, van den Bogert AJ. Horses damp the spring in their step. Nature. 2001; 414: 895–899.

[5] Silver FH, Siperko LM, Seehra GP. Mechanobiology of force transduction in dermal tissue. Skin Research and Technology. 2003; 9: 3–23.

[6] Silver FH, Kelkar N, Deshmukh T. Molecular Basis for Mechanical Properties of ECMs: Proposed Role of Fibrillar Collagen and Proteoglycans in Tissue Biomechanics. Biomolecules. 2021; 11: 1018.

[7] Silver FH, Bradica G, Tria A. Elastic energy storage in human articular cartilage: estimation of the elastic modulus for type II collagen and changes associated with osteoarthritis. Matrix Biology. 2002; 21: 129–137.

[8] Shah RG, DeVore D, Pierce MC, Silver FH. Vibrational analysis of implants and tissues: Calibration and mechanical spectroscopy of multi-component materials. Journal of Biomedical Materials Research Part A. 2017; 105: 1666–1671.

[9] Silver FH, Kelkar N, Deshmukh T, Horvath I, Shah RG. Mechano-Vibrational Spectroscopy of Tissues and Materials Using Vibrational Optical Coherence Tomography: a New Non-

Invasive and Non-Destructive Technique. Recent Progress in Materials. 2020; 2: 1–16.
[10] Crespo MA, Jimenez HJ, Deshmukh T, Pulido JS, Saad AS, Silver FH, *et al*. In Vivo Determination of the Human Corneal Elastic Modulus Using Vibrational Optical Coherence Tomography. Translational Vision Science & Technology. 2022; 11: 11.
[11] Silver F H, Shah R G, Silver LL. The use of vibrational optical coherence tomography in matching host tissue and implant mechanical properties. Biomaterials and Medical Applications. 2018; 2: 2.
[12] Silver FH, Kelkar N, Deshmukh T, Ritter K, Ryan N, Nadiminti H. Characterization of the Biomechanical Properties of Skin Using Vibrational Optical Coherence Tomography: Do Changes in the Biomechanical Properties of Skin Stroma Reflect Structural Changes in the Extracellular Matrix of Cancerous Lesions? Biomolecules. 2021; 11: 1712.
[13] Silver FH, Deshmukh T, Kelkar N, Ritter K, Ryan N, Nadiminti H. The "Virtual Biopsy" of Cancerous Lesions in 3D: Non-Invasive Differentiation between Melanoma and Other Lesions Using Vibrational Optical Coherence Tomography. Dermatopathology. 2021; 8: 539–551.
[14] Shah R G, Silver F H. Viscoelastic behavior of tissues and implant materials: Estimation of the elastic modulus and viscous contribution using optical coherence tomography and vibrational analysis. Journal of Biomedical Technology and Research, 2017; 3: 105–109.
[15] Sridhar M. Anatomy of cornea and ocular surface. Indian Journal of Ophthalmology. 2018; 66: 190.
[16] Crespo-Moral M, García-Posadas L, López-García A, Diebold Y. Histological and immunohistochemical characterization of the porcine ocular surface. PLoS ONE. 2020; 15: e0227732.
[17] Boote C, Sigal IA, Grytz R, Hua Y, Nguyen TD, Girard MJA. Scleral structure and biomechanics. Progress in Retinal and Eye Research. 2020; 74: 100773.
[18] Boote C, Kamma-Lorger C, Hayes S, Harris J, Burghammer M, Hiller J, *et al*. Quantification of Collagen Organization in the Peripheral Human Cornea at Micron-Scale Resolution. Biophysical Journal. 2011; 101: 33–42.
[19] Müller LJ, Pels E, Vrensen GF. The specific architecture of the anterior stroma accounts for maintenance of corneal curvature. British Journal of Ophthalmology 2001; 85: 437–443.
[20] Meek KM. Corneal collagen-its role in maintaining corneal shape and transparency. Biophysical Reviews. 2009; 1: 83–93.
[21] Watson PG, Young RD. Scleral structure, organisation and disease. A review. Experimental Eye Research. 2004; 78: 609–623.
[22] Dutton JJ. Anatomy of the Orbit. Radiology of the Orbit and Visual Pathways. Elsevier: USA. 2010.
[23] Man X, Arroyo E, Dunbar M, Reed DM, Shah N, Kagemann L, *et al*. Perilimbal sclera mechanical properties: Impact on intraocular pressure in porcine eyes. PLoS ONE. 2018; 13: e0195882.
[24] Van Buskirk EM. The anatomy of the limbus. Eye. 1989; 3: 101–108.
[25] Komai Y, Ushiki T. The three-dimensional organization of collagen fibrils in the human cornea and sclera. Investigative Ophthalmology and Visual Science. 1991; 32: 2244–2258.
[26] Seyed-Safi AG, Daniels JT. The limbus: Structure and function. Experimental Eye Research. 2020; 197: 108074.
[27] Park CY, Lee JK, Zhang C, Chuck RS. New Details of the Human Corneal Limbus Revealed with second Harmonic Generation Imaging. Investigative Opthalmology & Visual Science. 2015; 56: 6058.
[28] Hejtmancik JF, Shiels A. Overview of the Lens. Progress in Molecular Biology and Translational Science. 2015; 123: 119–127.
[29] Kardon R. Regulation of Light through the Pupil. Adler's Physiology of the Eye. 2011; 209: 502–525.
[30] Silver FH, Freeman JW, Seehra GP. Collagen self-assembly and the development of tendon mechanical properties. Journal of Biomechanics. 2003; 36: 1529–1553.